British Journal of Pharmacology (1998) 123, 1441–1449

Acetylcholine modulation of high-voltage-activated calcium channels in the neurones acutely dissociated from rat paratracheal ganglia

[1]Yoshinaka Murai, [1]Hitoshi Ishibashi, [1,3]Norio Akaike & [2]Yushi Ito

Departments of [1]Physiology and [2]Pharmacology, Faculty of Medicine, Kyushu University, Fukuoka 812-82, Japan

1 The modulation of high-voltage-activated (HVA) Ca^{2+} channels by acetylcholine (ACh) was studied in the paratracheal ganglion cells acutely dissociated from 2-week-old Wistar rats by use of the nystatin perforated patch recording configuration under voltage-clamp conditions.

2 ACh inhibited the HVA Ca^{2+} currents in a concentration- and voltage-dependent manner.

3 The inhibition was mimicked by a muscarinic agonist, oxotremorine. Pirenzepine and methoctramine produced parallel shifts to the right in the ACh concentration-response curves. Schild analysis of the ACh concentration-ratios yield pA_2 values for pirenzepine and methoctramine of 6.85 and 8.57, respectively, suggesting the involvement of an M_2 receptor.

4 Nifedipine, ω-conotoxin-GVIA and ω-conotoxin-MVIIC reduced the HVA I_{Ca} by 16.8, 59.2 and 6.3%, respectively. A current insensitive to all of these Ca^{2+} antagonists, namely 'R-type', was also observed. The results indicated the existence of L-, N-, P/Q-, and R-type Ca^{2+} channels.

5 The ACh-sensitive current component was markedly reduced in the presence of ω-conotoxin-GVIA, but not with both nifedipine and ω-conotoxin-MVIIC. ACh also inhibited the R-type HVA I_{Ca} remaining in saturating concentrations of nifedipine, ω-conotoxin-GVIA and ω-conotoxin-MVIIC.

6 The inhibitory effect of ACh was prevented by pretreatment with pertussis toxin.

7 It was concluded that ACh selectively reduces both the N- and R-type Ca^{2+} channels, by activating pertussis toxin sensitive G-protein through the M_2 muscarinic receptor in paratracheal ganglion cells.

Keywords: Rat airway; parasympathetic ganglia; Ca^{2+} channels; muscarinic receptors; perforated patch recording

Introduction

In the airway of mammals, the parasympathetic innervation is the predominant excitatory neuronal pathway, and the innervation is important for the regulation of airway smooth muscle tone, circulation, vascular permeability and mucous secretion (Smith & Taylor, 1971). The network of nerve fibres and a large number of ganglia situated on the serosal surface of the dorsal tracheal wall contributes to its innervation (Baker *et al*., 1986). Muscarinic receptors have been shown to be involved in the control of the airway function (Barnes, 1987). Molecular biological studies have confirmed the existence of at least five distinct subtypes (m1–m5) of muscarinic receptor genes (Bonner, 1989). The m1–m4 genes correspond most closely to the pharmacologically defined M_1–M_4 subtypes, respectively (Hulme *et al*., 1990; Lazareno *et al*., 1990). In the airway, there are two populations of muscarinic receptors at the neuro-effector junction, that is pre- and postjunctional receptors (muscarinic receptors) mediating the excitation from nerve to the airway smooth muscle cell. Acetylcholine (ACh) released from the nerve terminal activates the postjunctional receptors, and induces both a brief membrane depolarization, referred to as the excitatory junction potential (e.j.p.) (Ito & Tajima, 1981), and the breakdown of phosphoinositide to produce inositol 1,4,5-trisphosphate (IP_3) followed by muscle contraction (Hashimoto *et al*., 1985). Prejunctional muscarinic receptors (neuronal muscarinic receptors) attenuate the release of ACh from the vagus nerve terminals in the guinea-pig (Fryer & Maclagan, 1984; Kilbinger *et al*., 1991), rat (Zhu *et al*., 1977), dog (Ito & Yoshitomi, 1988) and man (Minette & Barnes, 1988). Thus it appears that the prejunctional inhibitory muscarinic autoreceptors play an important role as a 'braking system' in the cholinergic bronchoconstriction (Freyer & Maclagan, 1984; Ito & Yoshitomi, 1988). However, the mechanisms underlying the inhibitory effect of muscarinic agonists on ACh release in airway has yet to be clarified.

Voltage-gated Ca^{2+} channels contribute to the excitability of nerve cells and mediate the increase in presynaptic Ca^{2+} concentration which is necessary for neurotransmitter release. Mammalian neurones have been shown to express multiple types of pharmacologically distinct high-voltage-activated (HVA) Ca^{2+} channels (Ishibashi *et al*., 1995; Randall & Tsien, 1995). The recent molecular characterization and functional expression of Ca^{2+} channel clones from a variety of species have confirmed the existence of distinct L-, N-, P-, Q- and R-type channels (see Birnbaumer *et al*., 1994). ACh has been shown to inhibit HVA Ca^{2+} channels in rat hippocampal neurones (Gähwiler & Brown, 1987), rat basal forebrain neurones (Allen & Brown, 1993), rat sympathetic neurones (Bernheim *et al*., 1992) and NG108-15 cells (Caulfield & Brown, 1991). However, the direct effect of ACh on parasympathetic neurones from the paratracheal ganglia has not been elucidated. In the present study, therefore, we investigated the ACh action on HVA Ca^{2+} channels in acutely dissociated rat paratracheal ganglion cells, by use of the nystatin perforated patch clamp recording mode under voltage-clamp conditions.

Methods

Dissociation of paratracheal ganglion cells

The experiments were performed on the paratracheal ganglion cells freshly dissociated from 2-week-old Wistar rats. The

[3] Author for correspondence.

procedure for obtaining dissociated paratracheal ganglion cells is similar to that described elsewhere (Aibara *et al*., 1991). Briefly, the paratracheal ganglia were rapidly removed from the trachea of rats under ether anaesthesia, and then the ganglia were treated with a normal external solution containing 0.3% collagenase, 0.2% papain and 0.2% trypsin for 30 min at 35°C. Thereafter, the ganglion cells were dissociated mechanically by gentle pipetting in a culture dish. The dissociated cells adhered to the bottom of the dish within 20 min. Then, the cells were prepared for the electrophysiological experiments. The experiments with pertussis toxin (islet-activating-protein; IAP) were done on the dissociated ganglion cells pretreated with 500 ng ml^{-1} IAP for 6–8 h at 32°C.

Solutions and chemicals

The ionic composition of a normal external solution was (in mM): NaCl 150, KCl 5, $MgCl_2$ 1, $CaCl_2$ 2, N-2-hydroxyethylpiperazine-N′-2-ethanesulphonic acid (HEPES) 10 and glucose 10. The pH was adjusted to 7.4 with tris(hydroxymethyl) aminomethane (Tris-OH). The ionic composition of the solution for recording Ca^{2+} channel currents was (in mM): N-methyl-D-glucamine-Cl (NMG-Cl) 140, CsCl 5, $CaCl_2$ 5, $MgCl_2$ 1, HEPES 10 and glucose 10. The pH was adjusted to 7.4 with Tris-OH. The composition of patch-pipette (internal) solution was (in mM): Cs-methanesulphonate 100, CsCl 50 and HEPES 10. The pH was adjusted to 7.2 with Tris-OH. Nystatin was dissolved in methanol, resulting in a 10 mg/ml^{-1} stock solution and added to the internal solution at a final concentration of 400 $\mu g\ ml^{-1}$ just before use. A rapid application of external solution was performed with the 'Y-tube' technique described previously (Nakagawa *et al*., 1990). With this technique, external solution could be completely exchanged within 20 ms.

Drugs used in the present experiment were acetylcholine, collagenase, pirenzepine, methoctramine, nifedipine, nystatin and oxotremorine (Sigma), methoctramine (Research Biochemical International), trypsin (Difco), ω-conotoxin-GVIA and ω-conotoxin-MVIIC (Peptide Institute), and dibutyryl adenosine 3′ : 5′-cyclic monophosphate (dibutyryl-cyclic AMP) and papain (Wako).

Electrophysiological recordings

Electrical measurements were performed with the nystatin perforated patch recording mode (Akaike & Harata, 1994). Patch pipettes were prepared by a vertical micropipette puller (PB-7, Narishige, Tokyo). The resistance between the patch pipette filled with the internal solution and the reference electrode in the normal external solution was 2–4 MΩ. After stable perforated patch formation, the series resistance ranged from 7 to 18 MΩ and was compensated in the same manner as that explained by Llano *et al*. (1991). Ionic currents were measured with a patch clamp amplifier (EPC-7, List-Medical), low-pass filtered at 1 kHz (E-3201A, NF Electronic Instruments, Tokyo, Japan) and monitored on both a digital storage oscilloscope (VC-6025, Hitachi, Tokyo, Japan). The data were stored on magnetic tapes by use of a digital audio tape recorder (RE-130TE, TEAC, Tokyo) for subsequent computer analysis with the pCLAMP system (Axon Instruments). All currents were corrected for linear leak and capacitative currents by use of scaled currents for a 5–20 mV hyperpolarization from a holding potential. All experiments were carried out at room temperature (21–24°C). Experimental values are presented as mean ± s.e.mean. Statistical significance was determined by use of paired or unpaired Student's *t* test.

Results

Inhibition of HVA I_{Ca} by ACh

Neuronal Ca^{2+} channels have been shown to be classified into two subtypes including low-voltage-activated (LVA) and high-voltage-activated (HVA) Ca^{2+} channels. However, as previously described (Aibara *et al*., 1992), the LVA Ca^{2+} channel current was not observed in the present preparation (not shown). Therefore, the effects of ACh on HVA I_{Ca} evoked by a depolarizing step pulse from a holding potential (V_H) of −50 mV to +20 mV were examined. Application of ACh rapidly reduced the HVA I_{Ca}, and the current amplitude fully recovered after washout. There was little desensitization following several applications. The percentage inhibition values of HVA I_{Ca} at first and third application of 3×10^{-7} M ACh, as shown in Figure 1A, were 57.1 ± 3.5% and 56.4 ± 2.1% ($n = 4$), respectively.

To determine the voltage-dependence of the ACh-induced inhibition of HVA I_{Ca}, the current-voltage (*I*-V) relationships were constructed in the presence and absence of 10^{-7} M ACh (Figure 1B). Under control conditions the HVA I_{Ca} was activated at membrane potential more positive than −20 mV and reached a maximum amplitude at +20 mV. However, the inhibitory effects of 10^{-7} M ACh on the HVA I_{Ca} were reduced at positive membrane potentials. The inhibition ratios at +20 and +50 mV were 54.0 ± 5.2% ($n = 5$) and 36.7 ± 3.8% ($n = 5$), respectively. These values were significantly different ($P < 0.05$, paired *t* test).

The inhibitory effect of ACh on HVA I_{Ca} was concentration-dependent and was mimicked by a muscarinic agonist, oxotremorine (Figure 2). When the concentration-inhibition curves were constructed for ACh- and oxotremorine-induced inhibition of HVA I_{Ca} elicited by a depolarizing step pulse from a V_H of −50 mV to +20 mV, the inhibitory effects of these agonists were saturated at high concentrations. The half-maximum inhibitory concentration (IC_{50}), the Hill coefficient and the maximum inhibition were 5.32×10^{-8} M, 1.08 and 70.7 ± 7.5% ($n = 10$) for ACh and 7.84×10^{-8} M, 1.01 and 68.2 ± 4.4% ($n = 8$) for oxotremorine, respectively.

Effects of muscarinic antagonists

The pharmacological subtypes of muscarinic receptor underlying the inhibition of the Ca^{2+} channels were investigated by use of two selective antagonists, pirenzepine and methoctramine. These antagonists themselves had no effects on HVA I_{Ca} at the concentrations used in this study (not shown). Figure 3Aa shows the concentration-inhibition curves for the ACh-sensitive current component in the presence and absence of pirenzepine. Pirenzepine shifted the concentration-inhibition curve to the right without significantly changing the maximum Ca^{2+} current inhibition. The IC_{50} values for ACh-induced inhibition of HVA I_{Ca} under control and in the presence of 10^{-7}, 3×10^{-7} and 10^{-6} M pirenzepine were 5.32×10^{-8}, 1.75×10^{-7}, 4.82×10^{-7} and 1.08×10^{-6} M, respectively. The Schild plot constructed from these values yielded a pA_2 of 6.85 for pirenzepine. Methoctramine also shifted the concentration-response curve to the right without affecting the maximum Ca^{2+} current inhibition (Figure 3Ab). The IC_{50} values for ACh-induced inhibition of HVA I_{Ca} under control and in the presence of 3×10^{-8}, 10^{-7} and 3×10^{-7} M methoctramine were 5.32×10^{-8}, 4.08×10^{-7}, 8.35×10^{-7} and 3.99×10^{-6} M, respectively. The Schild plot yielded a pA_2 of 8.57 for methoctramine.

Involvement of G-proteins

G-proteins mediate the transmitter-induced inhibition of Ca^{2+} channels in a wide variety of neurones (Brown & Birnbaumer, 1990). Pertussis toxin (islet activating protein; IAP) has been shown to catalyze the ADP-ribosylation of Gi- and Go-type of G-proteins and to block the effects of substances that use these proteins as transducers (Gilman, 1987). To test the IAP sensitivity of the effect of ACh, the dissociated neurones were incubated for 6–8 h with or without 500 ng ml^{-1} IAP in the external solution at 32°C. In control cells without IAP treatment, the inhibition induced by 10^{-6} M ACh was

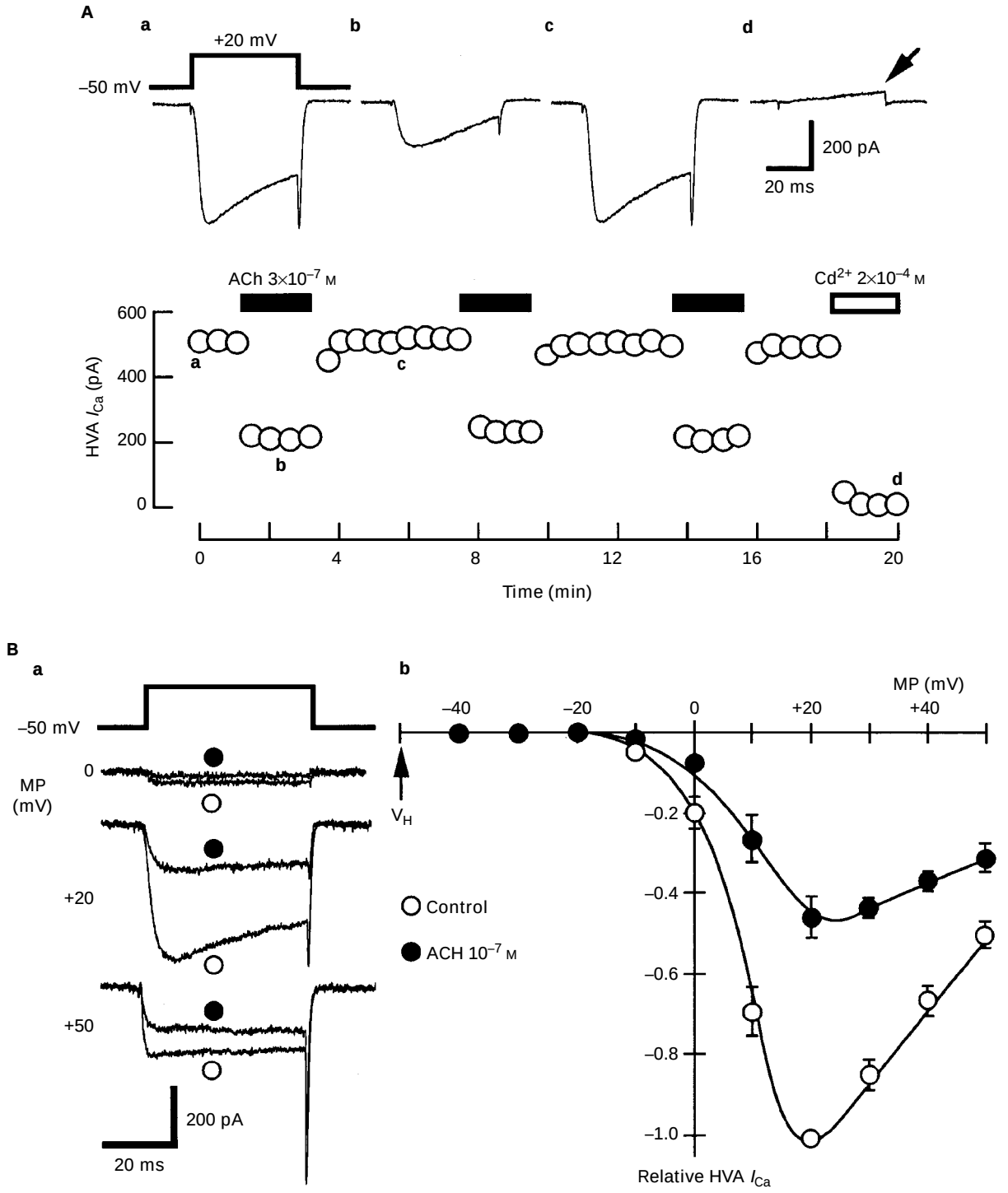

Figure 1 Effects of ACh on HVA I_{Ca}. (A) Time course of inhibition of peak HVA I_{Ca} evoked by a depolarizing step from a holding potential (V_H) of −50 mV to +20 mV every 30 s in the absence and presence (b) of 3×10^{-7} M ACh. The Cd^{2+}-insensitive leak current was also observed (arrow). In the presence of 2×10^{-4} M Cd^{2+}, current amplitudes were measured at a time when peak HVA I_{Ca} was observed under control conditions. (B) Voltage-dependence of ACh-induced inhibition of HVA I_{Ca} (a) Superimposed current traces obtained in the absence and presence of 10^{-7} M ACh at various membrane potentials (MP). The Cd^{2+} (2×10^{-4} M) insensitive leak (non-selective) current was subtracted from all current traces. (b) Current-voltage relationships in the absence and presence of ACh. The V_H was −50 mV. All current amplitudes were normalized to the peak current of control obtained at +20 mV. Each point represents the average of 5 neurones; vertical lines show s.e.mean.

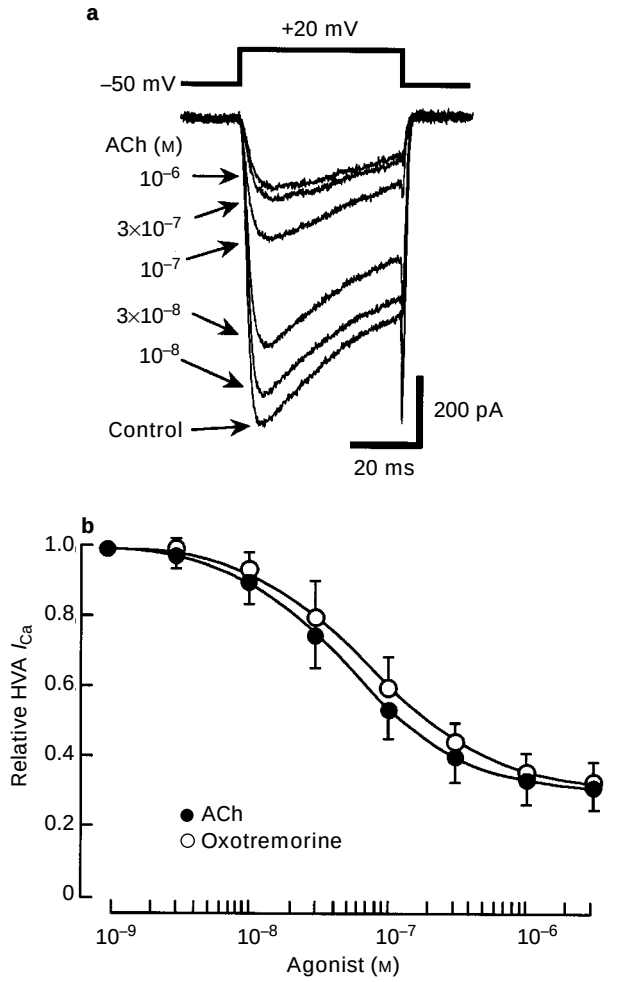

Figure 2 Effects of muscarinic agonists on HVA I_{Ca}. (a) HVA I_{Ca} in the absence and presence of various concentrations of ACh. HVA I_{Ca} was evoked by a depolarizing step from a V_H of -50 mV to $+20$ mV every 30 s. The Cd^{2+} (2×10^{-4} M)-insensitive leak current was subtracted from all current traces. (b) Concentration-inhibition curves for ACh and oxotremorine. The data were fitted to the logistic equation $I=1\text{-}(R_{max}xC^{n_H})/(C^{n_H}\text{-}IC_{50}{}^{n_H})$, where I is the normalized current amplitude, R_{max} is the maximum inhibition ratio, C is the agonist concentration, IC_{50} is the agonist concentration that produces 50% inhibition of the maximum response, and n_H is the Hill coefficient. Each point represents the average of 8–10 neurones; vertical lines show s.e.mean.

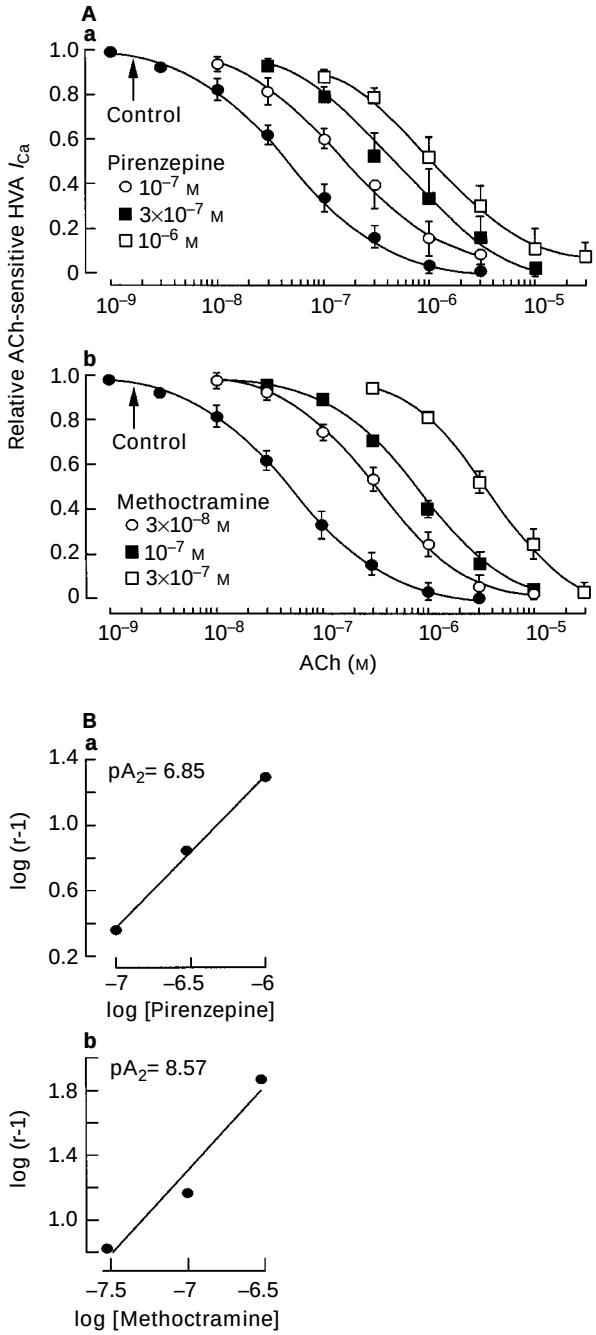

Figure 3 Effects of muscarinic antagonists on the ACh-induced inhibition of HVA I_{Ca}. (Aa) Concentration-response curves for inhibition of peak HVA I_{Ca} by ACh constructed under control conditions, and in the presence of 10^{-7} M, 3×10^{-7} M and 10^{-6} M pirenzepine. Each symbol represents the mean of 4–10 neurones. (b) Concentration-response curves for inhibition of peak HVA I_{Ca} by ACh constructed under control conditions, and in the presence of 3×10^{-8} M, 10^{-7} M and 3×10^{-7} M methoctramine. Each symbol represents the mean of 4–10 neurones. In (Aa and b) vertical lines show s.e.mean. (B) Schild analysis for these muscarinic antagonists. Schild plot was constructed from the data shown in (A), where r is the ACh concentration ratio. (a) The line was fitted by linear regression and yielded a pA_2 for pirenzepine of 6.85 with an unconstrained slope of 0.93 ($r^2=0.99$). (b) The line was fitted by linear regression and yielded a pA_2 for methoctramine of 8.57 with an unconstrained slope of 1.03 ($r^2=0.98$).

66.3±4.4% ($n=10$). In the IAP-treated neurones, the inhibition of HVA I_{Ca} by ACh was only 11.4±2.6% ($n=8$), as shown in Figure 4.

It is well known that Gi is coupled to adenylate cyclase (Gilman, 1987). However, pretreatment with dibutyryl-cyclic AMP (5×10^{-4} M, $n=4$), a membrane permeable cyclic AMP analogue, had no effect on either control HVA I_{Ca} or ACh-induced inhibition of HVA I_{Ca} (data not shown).

Effects of Ca^{2+} channel antagonists on HVA I_{Ca}

The effect of nifedipine, a dihydropyridine derivative, on HVA I_{Ca} is shown in Figure 5a. Nifedipine inhibited HVA I_{Ca} in a concentration-dependent manner, but its inhibitory effect was saturated at high concentrations more than 3×10^{-6} M. The IC_{50} value and maximum inhibition were 2.4×10^{-7} M and 14.8±0.7% ($n=5$), respectively.

The effect of ω-Cg-GVIA, a selective blocker of N-type Ca^{2+} channel, on HVA I_{Ca} evoked by a depolarizing step from a V_H of -50 mV to $+20$ mV was investigated. Figure 5b shows the time courses of development of the current inhibition by ω-Cg-GVIA at various concentrations. The

maximum inhibition of HVA I_{Ca} by ω-Cg-GVIA was $61.7 \pm 2.4\%$. The inhibition rate depended on the concentration of this toxin, and could be described by a single exponential function with time constants of 33, 72, 336 and 769 s for 3×10^{-6}, 10^{-6}, 3×10^{-7} and 10^{-7} M ω-Cg-GVIA, respectively. This indicates that ω-Cg-GVIA combines with a single binding site on the channel with a rate constant of about 1.2×10^4 s^{-1} m^{-1}. The rate constant is comparable to those in the chick dorsal root ganglion (DRG) neurones

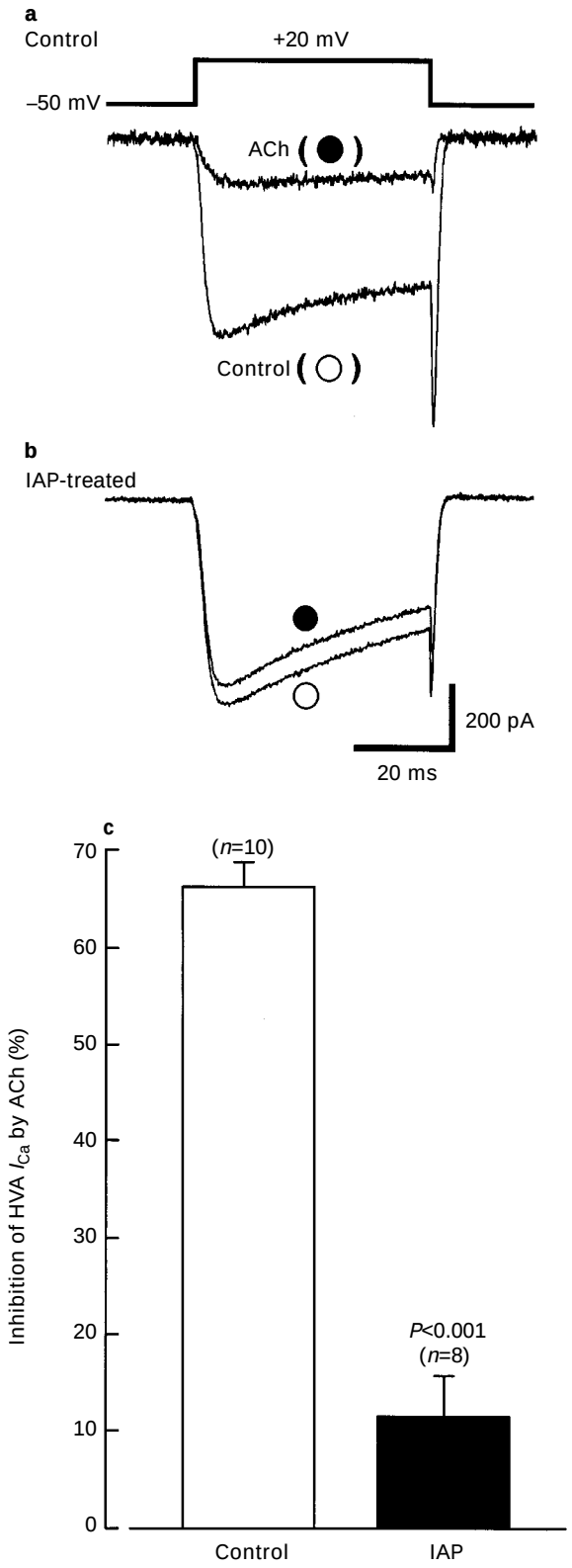

Figure 4 Effect of IAP on the ACh-induced inhibition of HVA I_{Ca}. (a) HVA I_{Ca} recorded in the absence and presence of 10^{-6} M ACh. The ganglion cells were immersed in the external solution without IAP for 6 h at 32°C. (b) Effect of 10^{-6} M ACh on HVA I_{Ca} of a neurone soaked in the external solution containing 500 ng ml^{-1} IAP for 6 h at 32°C. (c) Comparison of the 10^{-6} M ACh-induced inhibition of HVA I_{Ca} recorded from IAP-untreated ($n=10$) and IAP-treated neurones ($n=8$). Statistical comparison was performed with unpaired t test.

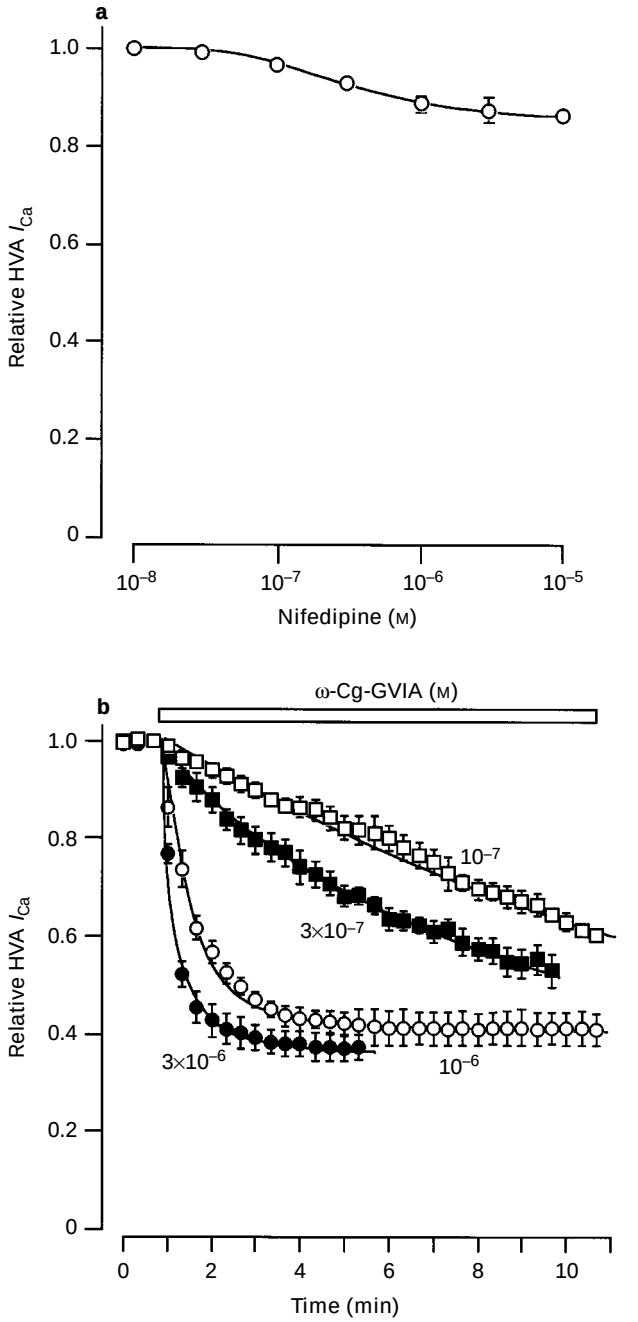

Figure 5 Effects of nifedipine and ω-Cg-GVIA on HVA I_{Ca}. HVA I_{Ca} was evoked by a depolarizing step from a V_H of -50 mV to $+20$ mV every 30 s. (a) Effect of nifedipine on HVA I_{Ca}. Each point represents the average of 5 ganglion cells. A smooth line was drawn according to equation: $I = 1\text{-}k/(1 + (IC_{50}/[ACh])^{n_H})$, where I represents relative amplitude, $IC_{50} = 2.4 \times 10^{-7}$ M and $k = 0.14$. (b) Effect of ω-Cg-GVIA. Time courses of the block of HVA I_{Ca} by ω-Cg-GVIA at four different concentrations (10^{-7}, 3×10^{-7}, 10^{-6} and 3×10^{-6} M). Smooth lines were drawn according to an equation: $I = k\exp(-\alpha[\omega\text{-Cg-GVIA}]t) + (1\text{-}k)$, where I represents relative HVA I_{Ca}. k amount of block and α an association rate constant. The values were $k = 0.59$ and $\alpha = 1.30 \times 10^4$ s^{-1} at 10^{-7}M, $k = 0.59$ and $\alpha = 1.00 \times 10^4$ s^{-1} at 3×10^{-7} M, $k = 0.61$ and $\alpha = 1.38 \times 10^4$ s^{-1} at 10^{-6} M, and $k = 0.64$ and $\alpha = 1.01 \times 10^4$ s^{-1} at 3×10^{-6} M.

(2×10^5 s^{-1} m^{-1} in a 2.5 mM Ba^{2+} solution, Aosaki & Kasai, 1989) and NG108-15 cells (1.7×10^4 s^{-1} m^{-1} in a 10 mM Ba^{2+} solution, Kasai & Neher, 1992). No recovery was detected up to 30 min after wash out (not shown).

Pharmacological separation of HVA Ca^{2+} channels

In the present study, HVA I_{Ca} was fractionated into N-, L-, P/Q- and R-type currents by the use of selective Ca^{2+} channel antagonists. The N- and L-type currents were defined as the currents blocked by 10^{-6} M ω-Cg-GVIA and 3×10^{-6} M nifedipine, respectively. The P/Q-type current was defined as that blocked by 3×10^{-6} M ω-Cm-MVIIC which blocks not only P/Q-type Ca^{2+} channels but also N-type channels (Randall & Tsien, 1995). As shown in Figure 6A and B, the successive reduction of the HVA I_{Ca} was observed with the cumulative application of these blockers at respective saturating concentrations. A residual current component (R-type current) remained in the presence of 10^{-6} M ω-Cg-GVIA, 3×10^{-6} M nifedipine and 3×10^{-6} M ω-Cm = MVIIC. The successive application of ω-Cm-MVIIC at 6×10^{-6} M had no further additional inhibition (data not shown), thereby suggesting that the concentration of ω-Cm-MVIIC (3×10^{-6} M) used is saturating. In 9 paratracheal ganglion cells, the total HVA I_{Ca} current consisted of $59.2 \pm 2.2\%$ N-type, $16.8 \pm 1.9\%$ L-type and $6.3 \pm 0.8\%$ P/Q-type and $19.3 \pm 1.4\%$ R-type HVA components (Figure 6C).

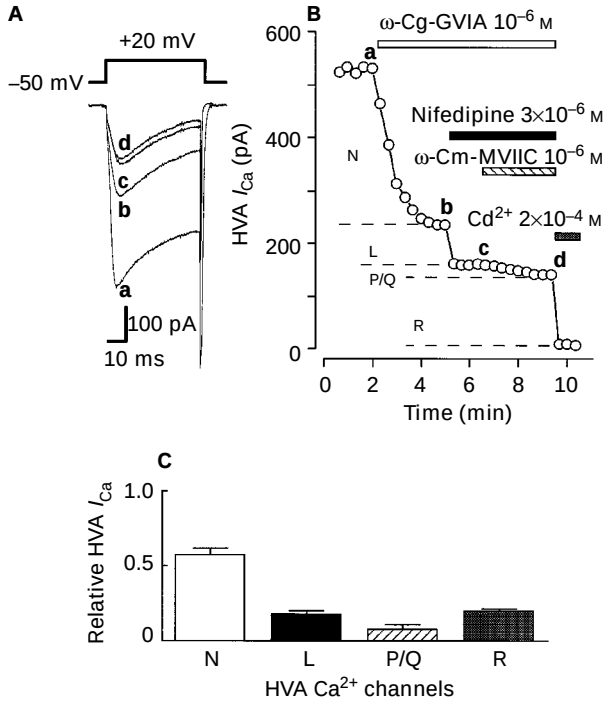

Figure 6 The pharmacological separation of the HVA I_{Ca}. (A) Superimposed current traces in control conditions and in the presence of selective Ca^{2+} antagonists which were applied cumulatively. Current traces (a–d) were obtained at a time indicated in (B), and the Cd^{2+} insensitive current was subtracted from all current traces. HVA I_{Ca} was evoked by a depolarizing step from a V_H of -50 mV to $+20$ mV every 30 s. (B) Time course of block of HVA I_{Ca} by Ca^{2+} antagonists. The data were obtained from the same cell shown in (A). (C) The fraction of HVA I_{Ca} contributed by the pharmacologically defined N-, L-, P/Q- and R-type Ca^{2+} channels. Each column represents the average of 9 neurones.

Selective inhibition of N- and R-type Ca^{2+} channels

To determine which subtypes of HVA Ca^{2+} channels in rat paratracheal ganglion cells are sensitive to ACh, the following experiments were performed. As shown in Figure 7A, block of L-type Ca^{2+} channel by nifedipine had little effect on the amount of current inhibited by ACh. The inhibition of HVA I_{Ca} by 3×10^{-7} M ACh in the absence and presence of nifedipine was 19.8 ± 2.6 pA pF^{-1} and 20.0 ± 2.8 pA pF^{-1} ($n = 5$), respectively. On the other hand, the continuous perfusion of ω-Cg-GVIA reduced the current inhibited by ACh (Figure 8A). The 3×10^{-7} M ACh-induced inhibition of

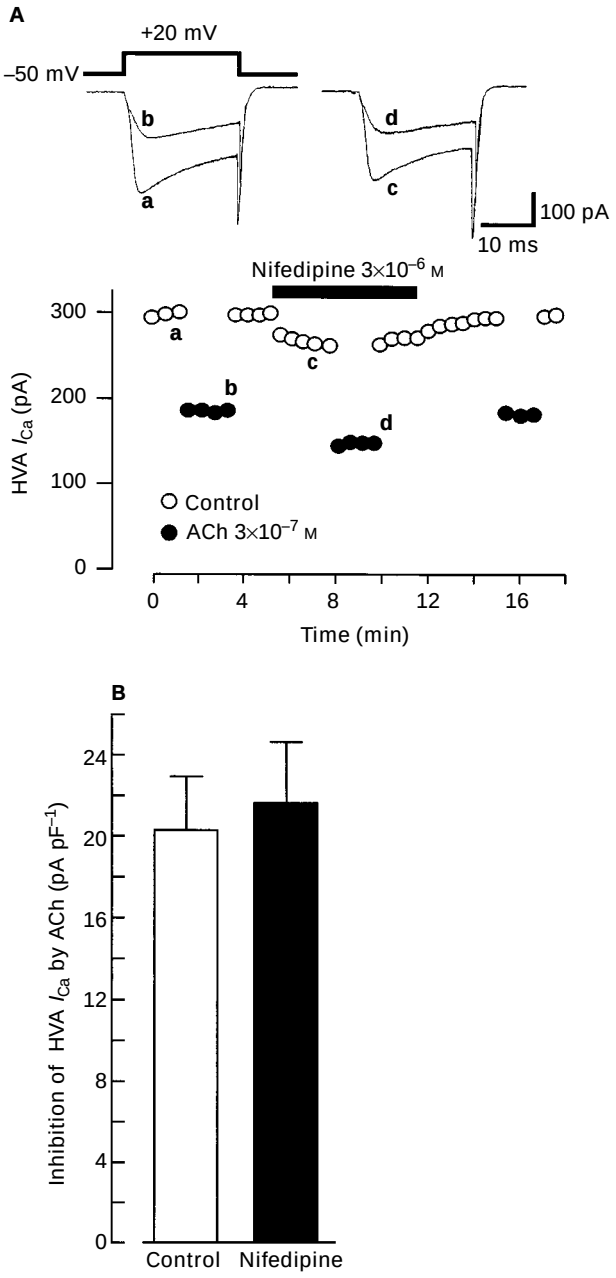

Figure 7 ACh-induced inhibition of HVA I_{Ca} was unaffected by nifedipine. (A) Current reduction produced by 3×10^{-7} M ACh in control conditions (upper left) and after block of L-type current with 3×10^{-6} M nifedipine (upper right). The Cd^{2+} insensitive current was subtracted from all current traces. Lower panel: corresponding time course. (B) Current reduction by ACh in control conditions and in the presence of nifedipine in 5 cells recorded as in (A). All currents were normalized to the cell capacitance.

HVA I_{Ca} was 18.3 ± 1.5 pA pF^{-1} in control and 5.4 ± 0.4 pA pF^{-1} after the blockade of N-type Ca^{2+} current by ω-Cg-GVIA ($n = 6$, Figure 8B). The subsequent application of 3×10^{-6} M ω-Cm-MVIIC ($n = 6$) had almost no effect on the amount of ACh-sensitive current, suggesting that P/Q-type Ca^{2+} channels are little involved in the ACh-induced inhibition of HVA I_{Ca}.

The inhibition of R-type channels by ACh was also investigated in a separate series of experiments. As shown in Figure 9, even in the presence of a saturating concentration of ω-Cg-GVIA, nifedipine and ω-Cm-MVIIC, the remaining HVA I_{Ca} was still inhibited by ACh by $63.0 \pm 5.4\%$ ($n = 6$). These results suggest that ACh selectively inhibits both N- and R-type HVA I_{Ca} components in the paratracheal ganglion cells.

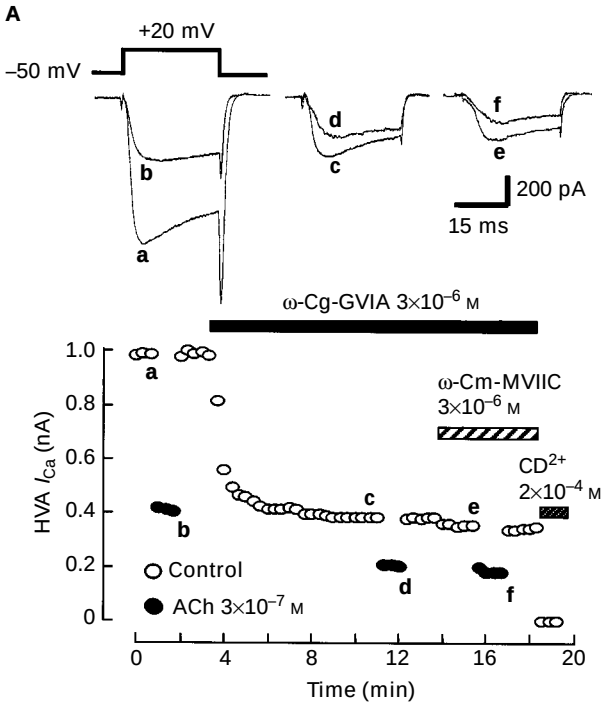

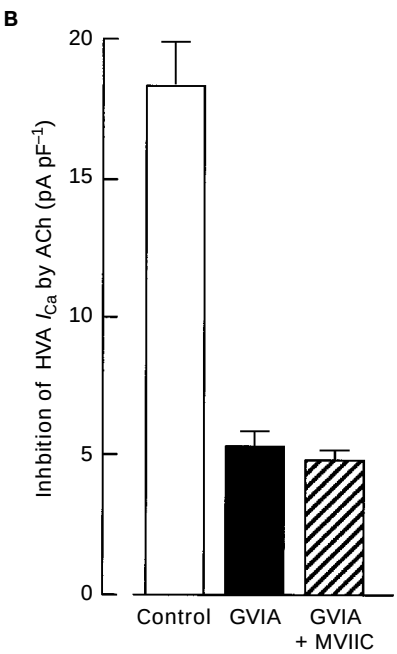

Figure 8 Effects of ω-Cg-GVIA and ω-Cm-MVIIC on ACh-induced inhibition of HVA I_{Ca}. (A) Current reduction produced by 3×10^{-7} M ACh in control conditions (upper left), after block of N-type current with 3×10^{-6} M ω-Cg-GVIA (upper middle) and after block of P/Q-type current with 3×10^{-6} M ω-Cm-MVIIC (upper right). The Cd^{2+} insensitive currents were subtracted from all current traces. Lower panel: corresponding time course. (B) Current reduction by ACh in control conditions and in the presence of Ca^{2+} antagonists in 6 cells recorded as in (A). Currents were normalized to cell capacitance.

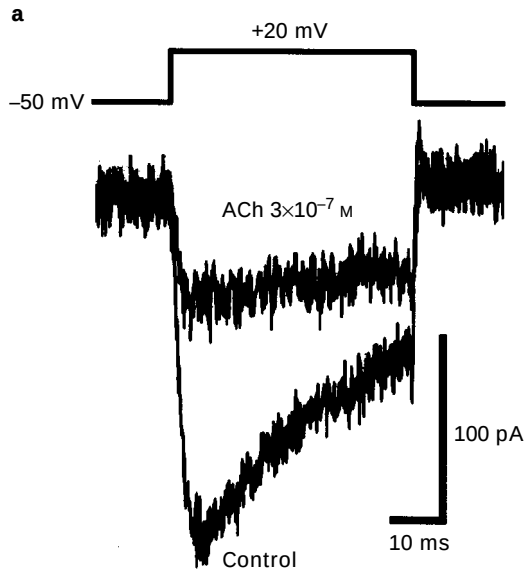

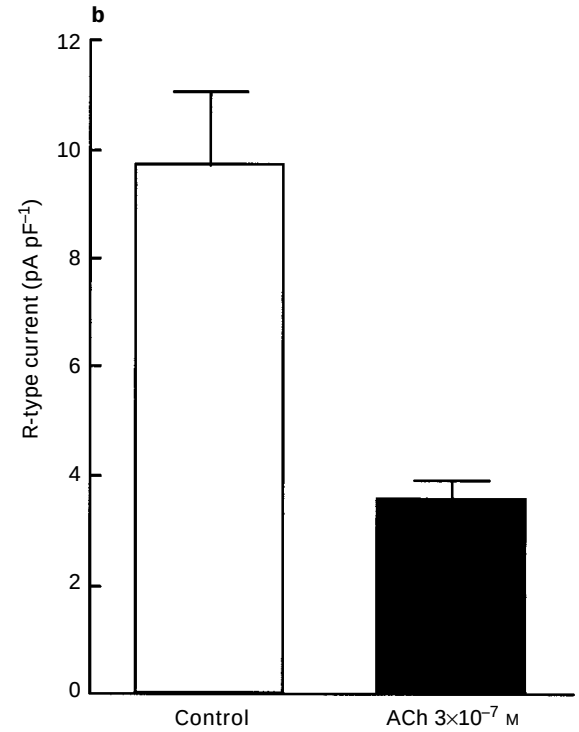

Figure 9 Effect of ACh on the R-type Ca^{2+} channel component. (a) Effect of 3×10^{-7} M ACh on the current remaining in the saturating concentration of nifedipine, ω-Cg-GVIA and ω-Cm-MVIIC. The Cd^{2+} insensitive currents were subtracted from all current traces. (b) HVA I_{Ca} in the absence and presence of ACh after block of L-, N- and P/Q-type Ca^{2+} currents. Currents were normalized to cell capacitance.

Discussion

Cholinergic nerves pass down the vagus nerve to synapse in ganglia in the airway wall, from which short postganglionic fibres contact airway smooth muscle cells. These release ACh, leading to contraction of the smooth muscle cells. Cholinergic nerves are the predominant neural pathway in the airways and cholinergic bronchoconstriction may be important in airway obstruction (Barnes *et al*., 1988). Thus, it seems that the modulatory mechanisms related to cholinergic bronchoconstriction play an important physiological role in the regulation of muscle tone in the airway. Prejunctional muscarinic autoinhibitory receptors, originally described in guinea-pig airway (Freyer & Maclagan, 1984), have also been identified in man, and were designated as muscarinic M_2-receptors in pharmacological studies with methoctramine and AF-DX (ten-Berge *et al*., 1996). Subsequent studies have shown that the profile might not be entirely consistent with activation of this subtype and indicate the presence of muscarinic M_4 rather than M_2 receptors (Kilbinger *et al*., 1995). However, primary cultures of parasympathetic neurones from guinea-pig trachea have recently been shown to express functional muscarinic M_2 but not M_4 receptors (Freyer *et al*., 1996), despite the atypical pharmacology described previously (Kilbinger *et al*., 1995).

In the present experiments, performed with freshly isolated paratracheal ganglia, pirenzepine and methoctramine produced parallel shifts of the inhibitory dose-response curve for the Ca^{2+}-current induced by ACh to the right. Schild plot analysis of the agonist concentration-ratios yield pA_2 values of 6.85 and 8.57 for pirenzepine and methoctramine, respectively. The low affinity for pirenzepine suggests any contribution of muscarinic M_1 receptors is unlikely, whilst the high affinity for methoctramine favours the involvement of muscarinic M_2 and/or M_4 receptors. The pA_2 values for these antagonists on paratracheal gangion cells are similar to those estimated by ligand binding studies on heterologously expressed M_2 receptors. The pK_i values for pirenzepine and methoctramine in these binding studies are $6.04-6.70$ and $7.88-8.44$, respectively (Buckley *et al*., 1989; Dörje *et al*., 1991). However, the present results do not exclude the possible involvement of muscarinic M_4 receptors, if any, in the inhibitory effects of ACh on the Ca^{2+}-current in the paratracheal ganglion cell.

Rat central and peripheral neurones have various populations of current corresponding to L-, N-, P-, Q- and R-type Ca^{2+} channels (Lipscombe *et al*., 1989; Ishibashi *et al*., 1995). In the present study, three different types of Ca^{2+} channel antagonists blocked the respective different components of whole-cell Ca^{2+} current in the cell bodies of paratracheal ganglion cells. ω-Cg-GVIA blocked the largest proportion of HVA Ca^{2+} currents (nearly 60%). Saturating doses of nifedipine and ω-Cm-MVIIC blocked about 15 and 6% of the whole-cell Ca^{2+} current, respectively. A strong effect of ω-Cg-GVIA on HVA Ca^{2+} channel currents, in addition to the small fractional inhibition of the HVA currents by dihydropyridines (DHPs), has also been observed in rat sympathetic ganglion cells (Lipscombe *et al*., 1989). The present experiments clearly indicated that ACh suppresses Ca^{2+} currents in the presence of nifedipine (3×10^{-6} M) to a similar extent in the control condition and that ω-Cg-GVIA (10^{-6} M) greatly reduces the ACh-sensitive Ca^{2+} current, indicating that the main channel component of ACh-sensitive Ca^{2+} currents is N-type. Furthermore, it is clear that ACh suppresses the R-type Ca^{2+} current, since ACh did suppress the residual Ca^{2+} current even after the treatment of ganglion cells with nifedipine, ω-Cg-GVIA and ω-Cg-MVIIC. Under the assumption that N- or R-type Ca^{2+} channels are present in the nerve terminals and that these receptors are coupled with muscarinic ACh-receptors through IAP-sensitive G-proteins, as observed in a cell body, the inhibition of these Ca^{2+} channels by ACh would reduce the amount of ACh released from the nerve terminals in response to single or repetitive stimulation in normal conditions.

Involvement of abnormalities in the autonomic nervous system in bronchial hyperresponsiveness has been proposed. Such abnormalities include the enhanced cholinergic (Simonsson *et al*., 1967) and α-adrenergic, or reduced β-adrenergic or NANC inhibitory mechanisms (Barnes, 1984; Szentivanyi, 1968). The lack of inhibitory mechanisms involved in the ACh output from the nerve terminal may be one of the factors involved in the enhanced cholinergic activity. Thus, it is reasonable to assume that the accelerated release of ACh resulting from changes in prejunctional modulation of transmitter release through muscarinic autoreceptors may be one of the mechanisms involved in the altered airway function in asthma (Barnes, 1987). The ACh release from the vagus nerve terminals is modulated in many ways, for example, by catecholamines, neuropeptides and autacoids, in addition to ACh itself. Prejunctional inhibition of ACh release from the vagal nerve terminals has been demonstrated for noradrenaline (Ito & Tajima, 1982), prostaglandin E series (for review see Ito, 1991) and nitric oxide (Jing *et al*., 1995; Tanaka *et al*., 1996), whereas the mediators such as histamine (Inoue & Ito, 1986) and substance P (Aizawa *et al*., 1990) have been shown to enhance ACh release by prejunctional mechanisms. It seems that in the airway 'braking systems for excitation' act through various endogenous substances and this is the dominat modulatory mechanism involved in neuro-effector transmission. Mainly because, (i) excitatory neurotransmitter ACh coexists with inhibitory neurotransmitters such as NO and vasoactive intestinal peptide (VIP) in the vagus nerve terminals, and the threshold for transmitter release is almost identical for NO and ACh. This means that ACh and NO are co-released and the released NO relaxes the airway smooth muscle, and there is evidence that endogenous NO inhibits ACh release from the nerve terminal, thus playing a 'double braking role' in cholinergic bronchoconstriction (Tanaka *et al*., 1996). (ii) It is generally considered that repetitive stimuli at low frequency induce the depression phenomena of e.j.p. in the airway smooth muscle which is due to ACh released from vagus nerve terminal, but facilitation in blood vessels or vas deferens which are innervated by sympathetic nervous system. These observations indicate that the parasympathetic nervous system operates under various kinds of 'braking system' in the airway, and breakdown of such a 'braking system' would bring the exaggerated cholinergic bronchoconstriction. The aspirin-sensitivity in asthmatic patients, for example, may correlate to the loss of modulatory actions of PGE series to inhibit ACh release from the nerve terminals (Ito, 1991). In addition to aspirin, other cyclo-oxygenase inhibitors including indomethacin have also been found to be linked to an acute asthmatic attack, in a patient with intrinsic bronchial asthma (Dawson & Sweatman, 1975). Autoregulation of the neurotransmitter release in the airway may be a physiological function and is probably an essential control mechanism of the excitatory cholinergic neuro-effector transmission.

This study was funded by grant-in-aid for Scientific Research (07407002) to N. A. and (80037506) to Y.I. from the Ministry of Education, Science and Culture, Japan and Mitsui Life Social Welfare Foundation.

References

AIBARA, K., EBIHARA, S. & AKAIKE, N. (1992). Voltage-dependent ionic currents in dissociated paratracheal ganglion cells of the rat. *J. Physiol.,* **457,** 591 – 610.

AIZAWA, H., MIYAZAKI, N., IOUE, H., IKEDA, T. & SHIGEMATSU, N. (1990). Effect of endogenous tachykinins on neuro-effector transmission of vagal nerve in guinea-pig tracheal tissue. *Respiration,* **57,** 338 – 342.

AKAIKE, N. & HARATA, N. (1994). Nystatin perforated patch recording and its applications to analysis of intracellular mechanisms. *Jap. J. Physiol.,* **44,** 433 – 473.

ALLEN, T.G.J. & BROWN, D.A. (1993). M_2-muscarinic receptor-mediated inhibition of the Ca^{2+} current in rat magnocellular cholinergic basal forebrain neurones. *J. Physiol.,* **466,** 173 – 189.

AOSAKI, T. & KASAI, H. (1989). Characterization of two kinds of high-voltage-activated Ca-channel currents in chick sensory neurons. *Pflügers Arch.,* **414,** 150 – 156.

BAKER, D.G., MCDONALD, D.M., BASBAUM, C.B. & MITCHELL, R.A. (1986). The architecture of nerves and ganglia of the ferret trachea as revealed by acetylcholinesterase histochemistry. *J. Comp. Neurol.,* **246,** 513 – 526.

BARNES, P.J. (1984). Adrenergic receptors of normal and asthmatic airways. *Eur. J. Respir. Dis. Suppl.,* **135,** 72 – 79.

BARNES, P.J. (1987). Cholinergic control of airway smooth muscle. *Am. Rev. Respir. Dis.,* **136,** S42 – S45.

BARNES, P.J., MINETTE, P. & MACLAGAN, J. (1988). Muscarinic receptor subtype in airways. *Trends Pharmacol. Sci.,* **9,** 412 – 416.

TEN-BERGE, R.E., ZAAGSMA, J. & ROFFEL, A.F. (1996). Muscarinic inhibitory autoreceptors in different generations of human airways. *Am. J. Respir. Crit. Care. Med.,* **154,** 43 – 49.

BERNHEIM, L., MATHIE, A. & HILLE, B. (1992). Characterization of muscarinic receptor subtypes inhibiting Ca^{2+} current and M current in rat sympathetic neurons. *Proc. Natl. Acad. Sci. U.S.A.,* **89,** 9544 – 9548.

BIRNBAUMER, K.P., CAMPBELL, K.P., CATTERALL, W.A., HARPOLD, M.M., HOFMANN, F., HORNE, W.A., MORI, Y., SCHWARTZ, A., SNUTCH, T.P., TANABE, T. & TSIEN, R.W. (1994). The naming of voltage-gated calcium channels. *Neuron,* **13,** 505 – 506.

BONNER, T.I. (1989). The molecular basis of muscarinic receptor density. *Trends Neurosci.,* **12,** 148 – 151.

BROWN, A.M. & BIRNBAUMER, L. (1990). Ionic channels and their regulation by G protein subunits. *Ann. Rev. Physiol.,* **52,** 197 – 213.

BUCKLEY, N.J., BONNER, T.I., BUCKLEY, C.M. & BRANN, M.R. (1989). Antagonist binding properties of five cloned muscarinic receptors expressed in CHO-K1 cells. *Mol. Pharmacol.,* **35,** 469 – 476.

CAULFIELD, M.P. & BROWN, D.A. (1991). Pharmacology of the putative M_4 muscarinic receptor mediating Ca-current inhibition in neuroblastoma x glioma hybrid (NG108-15) cells. *Br. J. Pharmacol.,* **104,** 39 – 44.

DAWSON, W. & SWEATMAN, W.J.F. (1975). Probable role of prostagrandins in asthma. *Int. Arch. Appl. Immunol.,* **49,** 213 – 216.

DÖRJE, F., WESS, J., LAMBRECHT, G., TACKE, R., MUTSCHLER, E. & BRANN, M.R. (1991). Antagonist binding profiles of five cloned human muscarinic receptor subtypes. *J. Pharmacol. Exp. Ther.,* **256,** 727 – 733.

FREYER, A.D., ELBON, C.L., KIM, A.L., XIAO, H.Q., LEVEY, A.I. & JACOBY, D.B. (1996). Cultures of airway parasympathetic nerves express functional M_2 muscarinic receptors. *Am. J. Respir. Cell. Mol. Biol.,* **15,** 716 – 725.

FREYER, A.D. & MACLAGAN, J. (1984). Muscarinic inhibitory receptors in pulmonary parasympathetic nerves in the guinea-pig. *Br. J. Pharmacol.,* **83,** 973 – 978.

GÄHWILER, B.H. & BROWN, D.A. (1987). Muscarine affects calcium-currents in rat hippocampal pyramidal cells in vitro. *Neurosci. Lett.,* **76,** 301 – 306.

GILMAN, A.G. (1987). G proteins: Transducers of receptor-generated signals. *Ann. Rev. Biochem.,* **56,** 615 – 649.

HASHIMOTO, T., HIRATA, M. & ITO, Y. (1985). A role for inositol 1,4,5-trisphosphate in the initiation of agonist-induced contraction of dog tracheal smooth muscle. *Br. J. Pharmacol.,* **86,** 191 – 199.

HULME, E.C., BIRDSALL, N.J.M. & BUCKLEY, N.J. (1990). Muscarinic receptor subtypes. *Ann. Rev. Pharmacol. Toxicol.,* **30,** 633 – 673.

INOUE, T. & ITO, Y. (1986). Characteristics of neuro-effector transmission in the smooth muscle layer of dog bronchiole and modifications by autacoids. *J. Physiol.,* **370,** 551 – 565.

ISHIBASHI, H., RHEE, J.S. & AKAIKE, N. (1995). Regional difference of high voltage-activated Ca^{2+} channels in rat CNS neurones. *NeuroReport,* **6,** 1621 – 1624.

ITO, Y. (1991). Prejunctional control of excitatory neuroeffector transmission by prostagrandins in the airway smooth muscle tissue. *Ann. Rev. Respir. Dis.,* **143,** S6 – S10.

ITO, Y. & TAJIMA, K. (1981). Spontaneous activity in the trachea of dogs treated with indomethacin: an experimental model for aspirin-related asthma. *Br. J. Pharmacol.,* **73,** 563 – 571.

ITO, Y. & TAJIMA, K. (1982). Dual effects of catecholamines on pre- and post-junctional membranes in the dog trachea. *Br. J. Pharmacol.,* **75,** 433 – 440.

ITO, Y. & YOSHITOMI, T. (1988). Autoregulation of acetylcholine release from vagus nerve terminals through activation of muscarinic receptors in the dog trachea. *Br. J. Pharmacol.,* **93,** 636 – 646.

JING, L., INOUE, R., TASHIRO, K., TAKAHASHI, S. & ITO, Y. (1995). Role of nitric oxide in non-adrenergic, non-cholinergic relaxation and modulation of excitatory neuro-effector transmission in the cat airway. *J. Physiol.,* **483,** 225 – 237.

KASAI, H. & NEHER, E. (1992). Dihydropyridine sensitive and ω-conotoxin-sensitive calcium channels in a mammalian neuroblastoma-glioma cell line. *J. Physiol.,* **448,** 161 – 188.

KILBINGER, H., VON-BARDELEBEN, R., SIEFKEN, H. & WOLF, D. (1995). Prejunctional muscarinic receptors regulating neurotransmitter release in airways. *Life Sci.,* **56,** 981 – 987.

KILBINGER, H., SCHNEIDER, R., SIEFKEN, H., WOLF, D. & D'AGONISTO, G.D. (1991). Characterization of prejunctional muscarinic auto receptors in the guinea-pig trachea. *Br. J. Pharmacol.,* **103,** 1757 – 1763.

LAZARENO, S., BUCKLEY, N.J. & ROBERTS, F.F. (1990). Characterization of muscarinic M_4 binding sites in rabbit lung, chicken heart and NG108-15 cell. *Mol. Pharmacol.,* **38,** 805 – 815.

LIPSCOMBE, D., KONGSAMUT, S. & TSIEN, R.W. (1989). α-Adrenergic inhibition of sympathetic neurotransmitter release mediated by modulation of N-type calcium channel. *Nature,* **340,** 639 – 642.

LLANO, I., MARTY, A., ARMSTRONG, C.M. & KONNERTH, A. (1991). Synaptic- and agonist-induced excitatory currents of Purkinje cells in rat cerebellar slices. *J. Physiol.,* **434,** 183 – 213.

MINETTE, P.A. & BARNES, P.J. (1988). Pre-junctional inhibitory muscarinic receptors on cholinergic nerves in human and guinea-pig airways. *J. Appl. Physiol.,* **64,** 2532 – 2537.

NAKAGAWA, T., SHIRASAKI, T., WAKAMORI, M., FUKUDA, A. & AKAIKE, N. (1990). Excitatory amino acid response in isolated nucleus tractus solitarii neurons of the rat. *Neurosci. Res.,* **8,** 114 – 123.

RANDALL, A. & TSIEN, R.W. (1995). Pharmacological dissection of multiple types of Ca^{2+} channel currents in rat cerebellar granule neurons. *J. Neurosci.,* **15,** 2995 – 3012.

SIMONSSON, B.G., JACOBS, F.M. & NADEL, J. (1967). Role of autonomic nervous system and the cough reflex in the increased responsiveness of airways in patients with obstructive airway disease. *J. Clin. Invest.,* **46,** 1812 – 1818.

SMITH, R.B., TAYLOR, I.M. (1971). Observations on the intrinsic innervation of trachea, bronchi, and pulmonary vessels in the sheep. *Acta Anatomica,* **80,** 1 – 13.

SZENTIVANYI, A. (1968). The beta adrenergic theory of the atopic abnormality in bronchial asthma. *J. Allergy,* **42,** 203 – 232.

TANAKA, H., JING, L., TAKAHASHI, S. & ITO, Y. (1996). The possible role of nitric oxide in relaxations and excitatory neuroeffector transmission in the cat airway. *J. Physiol.,* **493,** 785 – 791.

ZHU, F.-X., ZHANG, X.-Y. & ROBINSON, N.E. (1997). Origin and modulation of ACh release from rat airway cholinergic nerves. *Am. J. Physiol.,* **272,** L8 – L14.

(Received October 13, 1997
Revised December 16, 1997
Accepted December 23, 1997)